

Reducing Circuit Resources in Grover's Algorithm via Constraint-Aware Initialization

Eunok Bae,^{1,*} Jeonghyeon Shin,^{2,3} and Minjin Choi^{4,†}

¹ Electronics and Telecommunications Research Institute, Daejeon 34129, Republic of Korea

² Center for Quantum Technology, Korea Institute of Science and Technology, Seoul 02792, Republic of Korea

³ Department of Mathematics and Research Institute for Basic Sciences,

Kyung Hee University, Seoul 02447, Republic of Korea

⁴ Center for Quantum Information R&D, Korea Institute of Science and Technology Information, Daejeon 34141, Republic of Korea

(Dated: January 27, 2026)

Grover's search algorithm provides a quadratic speedup over classical brute-force search in terms of query complexity and is widely used as a versatile subroutine in numerous quantum algorithms, including those for combinatorial problems with large search spaces. For such problems, it is natural to reduce the effective search space by incorporating problem constraints at the initialization step, which in Grover's algorithm can be achieved by preparing structured initial states that encode constraint information. In this work, we present a systematic framework with a simple preprocessing procedure for constraint-aware initialization in Grover's algorithm, focusing on problems with linear constraints. While such structured initial states can reduce the number of oracle queries required to obtain a solution, their preparation incurs additional circuit-level costs. We therefore offer a conservative circuit-level resource analysis, showing that the resulting constraint-aware initialization can improve resource efficiency in terms of gate counts and circuit depth. The validity of the framework is further demonstrated numerically using the exact-cover problem. Overall, our results indicate that this approach serves as a practical baseline for achieving more resource-efficient implementations of Grover's algorithm compared to the standard uniform initialization.

I. INTRODUCTION

Grover's search algorithm is one of the most prominent quantum algorithms, offering a quadratic speedup over brute-force methods for unstructured search problems [1]. Beyond its original formulation, it has been widely recognized as a versatile component across a broad range of quantum algorithms. In particular, Grover's algorithm underlies amplitude amplification [2, 3] and has been adapted for quantum counting [4, 5]. It has also been extended from the minimum finding algorithm [6] to more general iterative search schemes for optimization, such as Grover adaptive search [7, 8]. Recent work has explored integrating Grover's algorithm with quantum machine learning, for example in robotic kinematic optimization, and has reported potential performance gains on practical high-dimensional instances [9]. This broad applicability highlights the role of Grover's algorithm not only as a breakthrough result in search problems but also as a foundational tool in quantum algorithm design.

Constraint satisfaction problems (CSPs), or more generally, combinatorial optimization problems (COPs) have been actively studied as natural targets for Grover-based approaches, with a steady stream of results reported in recent years [8, 10–14]. Since constraints are intrinsic to CSPs and ubiquitous in COPs, most Grover-based formulations incorporate them within the oracle, typically by penalizing constraint violations. While there have also been proposals to encode constraint information already in the initial state [15, 16], these approaches are often tailored to specific problems, and a systematic analysis of how constraint-aware initialization af-

fects resource requirements and performance remains relatively limited. This motivates a closer examination of initialization strategies that exploit available constraint structure beyond the oracle level.

In this work, we present a systematic framework with a simple preprocessing procedure for constraint-aware initialization in Grover's algorithm applied to combinatorial problems with linear constraints. Our approach introduces a classical preprocessing step that identifies jointly implementable constraint sets for initial state preparation, covering cardinality constraints realized by Dicke states [17] as well as parity-type information extracted from more general linear constraints. We incorporate this parity-type information via constructions based on Greenberger–Horne–Zeilinger (GHZ) states [18] expressed in the X basis (hereafter referred to as GHZ-type states). Such structured initialization can restrict the search to more relevant subspaces.

However, implementing constraint-aware initialization incurs additional circuit-level overhead, which motivates a careful resource analysis. We therefore provide a conservative circuit-level resource analysis of the proposed constraint-aware initialization. In this analysis, we focus on representative instances of our framework, namely the Dicke state with Hamming weight one and GHZ-type states, which capture the essential scaling behavior of cardinality and parity-type constraints. In particular, we examine how the number and size of disjoint constraint sets incorporated into the initial state affect gate counts and circuit depth, and show that the overall resource efficiency improves as additional disjoint sets are included. Even in the worst-case scenario where the preprocessing ultimately retains only a single constraint set, the resulting initialization strategy remains more resource-efficient than the standard uniform initialization. We further validate the proposed constraint-aware initialization scheme through numerical simulations on the exact-cover problem. The simulation

*Electronic address: eobae@etri.re.kr

†Electronic address: mathcmj89@gmail.com

results are consistent with our theoretical analysis, thereby providing numerical support for the proposed framework.

This paper is organized as follows. Section II introduces the proposed framework for constraint-aware initialization. Section III presents the theoretical and numerical analyses, and discusses the results. Finally, Section IV concludes the paper.

II. METHODS

A. Grover's algorithm with constraint-aware initialization

We consider the problem of identifying an unknown binary string $x \in \{0, 1\}^n$, where $n \in \mathbb{N}$, that satisfies a given condition, typically encoded as a Boolean function $f : \{0, 1\}^n \rightarrow \{0, 1\}$. The goal is to find a binary string x such that $f(x) = 1$.

Let $F \subseteq \{0, 1\}^n$ denote the search space. In the standard Grover's algorithm, F corresponds to the full search space $\{0, 1\}^n$. For the constraint-aware case considered in this work, F denotes a reduced subspace obtained by incorporating some or all of the problem's constraints, such that the subspace F includes the set of all solutions S . The initial state is then prepared as a uniform superposition over all binary strings in F as

$$\begin{aligned} |\psi_F^{(0)}\rangle_{\mathbf{q}_{[n]}} &= V_F |00 \cdots 0\rangle_{\mathbf{q}_{[n]}} \\ &= \frac{1}{\sqrt{|F|}} \sum_{x \in F} |x\rangle_{\mathbf{q}_{[n]}}, \end{aligned} \quad (1)$$

where $\mathbf{q}_{[n]} = q_1 q_2 \cdots q_n$ and V_F is a unitary operator that generates the desired superposition. For the full search space $F = \{0, 1\}^n$, V_F reduces to $H_{q_1} \otimes H_{q_2} \otimes \cdots \otimes H_{q_n}$, where H is the Hadamard operator. We define the solution and non-solution states as

$$|\phi_s\rangle_{\mathbf{q}_{[n]}} = \frac{1}{\sqrt{|S|}} \sum_{x \in S} |x\rangle_{\mathbf{q}_{[n]}} \quad (2)$$

and

$$|\phi_{ns,F}\rangle_{\mathbf{q}_{[n]}} = \frac{1}{\sqrt{|F| - |S|}} \sum_{x \in F \setminus S} |x\rangle_{\mathbf{q}_{[n]}}, \quad (3)$$

respectively. Then, the initial state can be expressed as a linear combination of these two orthonormal components as

$$|\psi_F^{(0)}\rangle_{\mathbf{q}_{[n]}} = \sin \theta |\phi_s\rangle_{\mathbf{q}_{[n]}} + \cos \theta |\phi_{ns,F}\rangle_{\mathbf{q}_{[n]}}, \quad (4)$$

where $\theta = \arcsin(\sqrt{|S|/|F|})$.

The overall procedure of Grover's algorithm consists of preparing the initial state, repeatedly applying the oracle and diffusion operators for an appropriate number of iterations, and finally measuring the state in the computational basis, as illustrated in Figure 1. The oracle operator O_f marks the solutions by flipping their phase:

$$O_f |x\rangle_{\mathbf{q}_{[n]}} = (-1)^{f(x)} |x\rangle_{\mathbf{q}_{[n]}}. \quad (5)$$

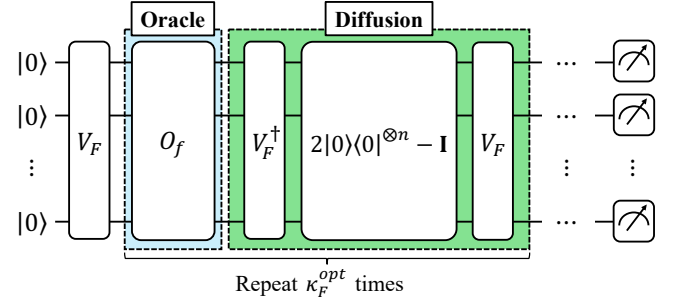


FIG. 1: Schematic of Grover's algorithm with constraint-aware initialization. The initial state $|\psi_F^{(0)}\rangle = V_F |0\rangle^{\otimes n}$ is a uniform superposition over the search subspace F , which may encode some or all of the problem's constraints. Each query consists of applying the oracle operator O_f followed by the diffusion operator $R_F = V_F(2|0\rangle\langle 0| - I)V_F^\dagger$. After κ_F^{opt} queries, a solution can be obtained with high probability upon measurement.

The diffusion operator is defined as a reflection about the initial state:

$$R_F = 2 |\psi_F^{(0)}\rangle\langle\psi_F^{(0)}|_{\mathbf{q}_{[n]}} - \mathbf{I}_{\mathbf{q}_{[n]}}, \quad (6)$$

where \mathbf{I} is the identity operator. We refer to the process of applying the oracle operator followed by the diffusion operator as a query. After performing κ queries starting from the initial state, the quantum state becomes

$$\begin{aligned} |\psi_F^{(\kappa)}\rangle_{\mathbf{q}_{[n]}} &= (R_F \cdot O_f)^\kappa |\psi_F^{(0)}\rangle_{\mathbf{q}_{[n]}} \\ &= \sin((2\kappa + 1)\theta) |\phi_s\rangle_{\mathbf{q}_{[n]}} + \cos((2\kappa + 1)\theta) |\phi_{ns,F}\rangle_{\mathbf{q}_{[n]}}. \end{aligned} \quad (7)$$

To maximize the amplitude of the solution state $|\phi_s\rangle$, κ is chosen such that $(2\kappa + 1)\theta \approx \pi/2$. As $\theta = \arcsin(\sqrt{|S|/|F|})$, we define the optimal number of queries as

$$\kappa_F^{opt} = \text{round}\left(\frac{\pi}{4 \arcsin(\sqrt{|S|/|F|})} - \frac{1}{2}\right). \quad (8)$$

In other words, after κ_F^{opt} queries, measuring the final state in the computational basis yields a solution with high probability.

B. Constraint-aware initialization for cardinality constraints

We first consider a class of linear constraints frequently encountered in combinatorial problems, known as cardinality constraints. Such constraints restrict the Hamming weight (the number of ones) of a subset of binary variables and can be written as

$$\sum_{i \in C_j} x_i = b_j, \quad j = 1, \dots, m, \quad (9)$$

where $C_j \subseteq \{1, \dots, n\}$ denotes the subset of variable indices associated with the j -th constraint, $x_i \in \{0, 1\}$, and $b_j \in \mathbb{N}$.

This simple yet important form arises in a variety of combinatorial problems, including the exact-cover problem [19–21] and the traveling salesman problem [22–24].

In the standard Grover's algorithm, such constraints are typically handled by the oracle, while the initial state is prepared as a uniform superposition over all 2^n binary strings. Here, we instead incorporate some of the constraints in Eq. (9) directly into the initial state, so that the search space is reduced to the set of basis states satisfying those constraints. We describe how this constraint-aware initialization can be realized using structured quantum states.

To illustrate the idea, let us examine a single cardinality constraint, which requires that the sum of the binary variables in a subset $C \subseteq \{1, \dots, n\}$ equals b . This constraint enforces that exactly b of the variables indexed by C are set to one. A natural way to reflect this constraint in the initial state is to prepare a Dicke state $|D_b^{|C|}\rangle$ on the corresponding qubits, where $|C|$ is the size of the subset C . A Dicke state $|D_v^\mu\rangle$ is defined as the equal superposition of all computational basis states of length μ with Hamming weight exactly v :

$$|D_v^\mu\rangle = \frac{1}{\sqrt{\binom{\mu}{v}}} \sum_{\substack{x \in \{0,1\}^\mu \\ \text{wt}(x)=v}} |x\rangle, \quad (10)$$

where $\text{wt}(x)$ is the Hamming weight of the binary string x . Dicke states can be prepared deterministically without ancillary qubits using the method proposed by Bärtschi and Eidenbenz [25], which requires $O(\mu v)$ gates and $O(\mu)$ circuit depth. This indicates that employing Dicke states for constraint-aware initialization can be achieved with reasonable circuit resources.

Given a set of cardinality constraints of the form in Eq. (9), one can in principle construct the initial state by preparing independent Dicke states on disjoint subsets of qubits corresponding to those constraints, while applying Hadamard gates to the remaining qubits. If a collection of disjoint subsets $\{C'_1, \dots, C'_t\}$ can be identified, the resulting initial state can be written, after an appropriate reordering of qubit indices, as

$$|\psi_F^{(0)}\rangle_{\mathbf{q}_{[n]}} = |D_{b'_1}^{|C'_1} \rangle_{\mathbf{q}_{C'_1}} \otimes \cdots \otimes |D_{b'_t}^{|C'_t} \rangle_{\mathbf{q}_{C'_t}} \otimes H|0\rangle_{q_{\gamma_t+1}} \otimes \cdots \otimes H|0\rangle_{q_n}, \quad (11)$$

where \mathbf{q}_Λ represents the set of qubits associated with the indices in a subset Λ , and $\gamma_t = \sum_{j=1}^t |C'_j|$ is the total number of qubits involved in the preparation of Dicke states. This construction reduces the search space size from 2^n to $2^{n-\gamma_t} \cdot \prod_{j=1}^t \binom{|C'_j|}{b'_j}$. In practice, identifying an optimal collection of disjoint subsets $\{C'_j\}$ that maximizes this reduction is itself a combinatorial problem and can be nontrivial. Nevertheless, a simple greedy procedure in Algorithm 1 can efficiently produce a feasible disjoint subset structure. The constraints are first sorted in ascending order of $\binom{|C_j|}{b_j}/2^{|C_j|}$, so that those imposing the strongest restriction on the feasible search space are prioritized. The algorithm then iteratively selects non-overlapping subsets, corresponding to the case where the overlap threshold is set to $\eta_{\text{th}} = 0$. This preprocessing step requires a classical cost of $O(mk)$, in addition to an initial sorting

Algorithm 1 Classical preprocessing for constraint-aware initialization with cardinality constraints

```

1: Input: Collection of pairs  $\{(C_j, b_j)\}_{j=1}^m$ ; overlap threshold  $\eta_{\text{th}}$ 
2: Output: Selected subset collection  $\mathcal{T}$ 
3:  $\mathcal{T} \leftarrow \emptyset, C_{\text{used}} \leftarrow \emptyset$ 
4:  $\mathcal{L} \leftarrow \{C_j\}_{j=1}^m$  sorted in ascending order of  $\binom{|C_j|}{b_j}/2^{|C_j|}$ 

Phase 1 (disjoint)
5: for each  $C_j$  in  $\mathcal{L}$  do
6:   if  $C_j \cap C_{\text{used}} = \emptyset$  then
7:      $\mathcal{T} \leftarrow \mathcal{T} \cup \{C_j\}$ 
8:      $C_{\text{used}} \leftarrow C_{\text{used}} \cup C_j$ 
9:   end if
10: end for

Phase 2 (overlap)
11: if  $\eta_{\text{th}} > 0$  then
12:    $\mathcal{R} \leftarrow \{C_j \in \mathcal{L} : C_j \notin \mathcal{T}\}$ 
13:   for each  $C_j$  in  $\mathcal{R}$  do
14:      $r \leftarrow |C_j \cap C_{\text{used}}|$ 
15:     if  $r \leq \eta_{\text{th}}$  then
16:        $R_j \leftarrow C_j \setminus C_{\text{used}}$ 
17:       if  $|R_j| > 0$  then
18:          $\mathcal{T} \leftarrow \mathcal{T} \cup \{R_j\}$ 
19:          $C_{\text{used}} \leftarrow C_{\text{used}} \cup R_j$ 
20:       end if
21:     end if
22:   end for
23: end if
24: return  $\mathcal{T}$ 

```

cost of $O(m \log m)$, where m is the number of constraints and k denotes the typical subset size.

The above construction considers only the case where the selected subsets are mutually disjoint. In many practical settings, however, constraints may share a number of common variables. To handle such cases, the greedy preprocessing can be extended to allow small overlaps among subsets. As described in the second phase of Algorithm 1, subsets whose overlap with the already selected ones is below a chosen threshold η_{th} are sequentially included after removing the shared elements. This additional phase involves only local overlap checks between subsets and thus requires the same classical cost of $O(mk)$ as in the disjoint case. Here, we denote by C_{used} the set of variable indices that have already been included in previously selected subsets. For a constraint subset C_j overlapping with C_{used} by $r_j = |C_j \cap C_{\text{used}}| \leq \eta_{\text{th}}$, we define the reduced set $R_j = C_j \setminus C_{\text{used}}$ and relax the corresponding cardinality constraint to

$$\max(0, b_j - r_j) \leq \sum_{i \in R_j} x_i \leq b_j. \quad (12)$$

This relaxed form defines a valid subspace over the remaining variables without conflicting with the original constraint. The corresponding quantum state is a superposition of Dicke states over the allowed Hamming weights,

$$|D_{b_j, r_j}^{|R_j|}\rangle = \frac{1}{\sqrt{\Omega_j}} \sum_{v=b_j^{\min}}^{b_j} \sqrt{\binom{|R_j|}{v}} |D_v^{|R_j|}\rangle, \quad (13)$$

where $b_j^{\min} = \max(0, b_j - r_j)$ and $\Omega_j = \sum_{v=b_j^{\min}}^{b_j} \binom{|R_j|}{v}$. Preparing a linear combination of Dicke states of the form $\sum_v \alpha_v |D_v^{\mu}\rangle$ can be implemented with $O(\mu^2)$ gates and $O(\mu)$ depth [25].

In summary, after preprocessing the constraints and re-ordering the qubit indices, the initial state can be constructed in the product form

$$\begin{aligned} |\psi_F^{(0)}\rangle_{q_{[n]}} &= |D_{b'_1}^{|C'_1|}\rangle_{q_{C'_1}} \otimes \cdots \otimes |D_{b'_t}^{|C'_t|}\rangle_{q_{C'_t}} \\ &\otimes |D_{b'_{t+1}, r'_{t+1}}^{|R'_{t+1}|}\rangle_{q_{R'_{t+1}}} \otimes \cdots \otimes |D_{b'_s, r'_s}^{|R'_s|}\rangle_{q_{R'_s}} \\ &\otimes H|0\rangle_{q_{\gamma_s+1}} \otimes \cdots \otimes H|0\rangle_{q_n}, \end{aligned} \quad (14)$$

where γ_s is the total number of qubits involved in the preparation of Dicke states and their linear combinations. As a result, the effective search space size is reduced from 2^n to $2^{n-\gamma_s} \cdot \prod_{j=1}^t \binom{|C'_j|}{b'_j} \cdot \prod_{j=t+1}^s \Omega_j$. Although more general, non-product forms of initialization are conceivable, the product structure in Eq. (14) offers a practical advantage. It provides a systematic and modular framework for embedding multiple constraints while keeping the circuit depth proportional to the largest subset size. Consequently, this approach enables constraint-aware initialization with relatively shallow depth while encoding some of the constraints, and can reduce both the effective search space and the overall circuit-level resource requirements of Grover's algorithm, as will be demonstrated in the Results and Discussion section.

C. Constraint-aware initialization for parity-type constraints

We next examine a more general linear constraint of the form

$$\sum_{i \in C} \alpha_i x_i = b, \quad (15)$$

where $C \subseteq \{1, \dots, n\}$, $x_i \in \{0, 1\}$, and $\alpha_i, b \in \mathbb{Z}$. Without loss of generality, we assume that the greatest common divisor of all coefficients $\{\alpha_i\}_{i \in C}$ and b is one. In contrast to the cardinality constraint discussed in the previous subsection, the number of ones among $\{x_i\}_{i \in C}$ cannot be predetermined in this case. Thus, the method based on the Dicke state is not applicable. To construct a feasible initialization in this setting, we instead exploit the parity structure of the coefficients. Let $\hat{C} = \{i \in C \mid \alpha_i \text{ is odd}\}$. By reducing Eq. (15) modulo 2, we obtain

$$\sum_{i \in \hat{C}} x_i \equiv b \pmod{2}, \quad (16)$$

which implies that if b is even (odd), then the number of ones among $\{x_i\}_{i \in \hat{C}}$ must also be even (odd). This parity condition can be encoded using a GHZ-type entangled state of the form

$$\begin{aligned} |GHZ_{\mu, v}^{(X)}\rangle &= \frac{1}{\sqrt{2}} (|+\rangle^{\otimes \mu} + (-1)^v |-\rangle^{\otimes \mu}) \\ &= \frac{1}{\sqrt{2^{\mu-1}}} \sum_{\substack{x \in \{0, 1\}^\mu \\ \text{wt}(x) \equiv v \pmod{2}}} |x\rangle, \end{aligned} \quad (17)$$

Algorithm 2 Classical preprocessing for constraint-aware initialization with general linear constraints

```

1: Input: Collection of triples  $\{(C_j, \{\alpha_{j,i}\}_{i \in C_j}, b_j)\}_{j=1}^m$ 
2: Output: Selected subset collection  $\mathcal{T}$ 
3:  $\mathcal{T} \leftarrow \emptyset, C_{\text{used}} \leftarrow \emptyset$ 
4: for  $j = 1, \dots, m$  do
5:    $\hat{C}_j \leftarrow \{i \in C_j : \alpha_{j,i} \text{ is odd}\}$ 
6: end for
7:  $\mathcal{L} \leftarrow \{\hat{C}_j\}_{j=1}^m$  sorted in ascending order of  $|\hat{C}_j|$ 
(Disjoint subset selection)
8: for each  $\hat{C}_j$  in  $\mathcal{L}$  do
9:   if  $\hat{C}_j \cap C_{\text{used}} = \emptyset$  then
10:     $\mathcal{T} \leftarrow \mathcal{T} \cup \{\hat{C}_j\}$ 
11:     $C_{\text{used}} \leftarrow C_{\text{used}} \cup \hat{C}_j$ 
12:   end if
13: end for
14: return  $\mathcal{T}$ 

```

where $|\pm\rangle = \frac{1}{\sqrt{2}}(|0\rangle \pm |1\rangle)$, $\mu \in \mathbb{N}$, and $v \in \{0, 1\}$. In the present setting, we set $\mu = |\hat{C}|$ and take $v = b \pmod{2}$, reflecting the parity condition in Eq. (16).

Now suppose that a set of linear constraints of the form

$$\sum_{i \in C_j} \alpha_{j,i} x_i = b_j, \quad j = 1, \dots, m, \quad (18)$$

is given, where, for each j , the coefficients $\{\alpha_{j,i}\}$ and b_j have the greatest common divisor one. Each constraint induces a parity condition on the subset $\hat{C}_j = \{i \in C_j \mid \alpha_{j,i} \text{ is odd}\}$. If one can identify disjoint subsets $\{\hat{C}'_1, \dots, \hat{C}'_t\}$, then, after reordering the qubit indices, the initial state can be written as

$$\begin{aligned} |\psi_F^{(0)}\rangle_{q_{[n]}} &= |GHZ_{|\hat{C}'_1|, b'_1}^{(X)}\rangle_{q_{\hat{C}'_1}} \otimes \cdots \otimes |GHZ_{|\hat{C}'_t|, b'_t}^{(X)}\rangle_{q_{\hat{C}'_t}} \\ &\otimes H|0\rangle_{q_{\gamma_t+1}} \otimes \cdots \otimes H|0\rangle_{q_n}, \end{aligned} \quad (19)$$

where $\hat{\gamma}_t = \sum_{j=1}^t |\hat{C}'_j|$ denotes the total number of qubits involved in the parity encoding. Since each constraint effectively reduces the search space by half, the resulting search space size becomes $2^{n-\hat{\gamma}_t}$, independent of the subset sizes $|\hat{C}_j|$. To maximize the overall reduction, it is therefore desirable to identify as many disjoint subsets as possible. To this end, we employ a simple greedy preprocessing procedure that iteratively selects disjoint parity subsets in ascending order of their sizes, as described in Algorithm 2.

When both cardinality and parity-type constraints are present, the initialization can be systematically constructed by combining Dicke states and GHZ-type states. Since encoding a cardinality constraint on a subset C_j via Dicke state preparation reduces the search space by a factor of $\binom{|C_j|}{b_j}/2^{|C_j|}$, whereas each parity-type constraint reduces it by exactly one half under the proposed initialization scheme, it can be advantageous in terms of search space reduction to prioritize subsets associated with cardinality constraints before applying the parity-based selection to the remaining constraints. This ordering enables an efficient reduction of the overall search space within a systematic framework.

III. RESULTS AND DISCUSSION

A. Resource requirement analysis

We evaluate the overall resource requirements associated with the constraint-aware initialization considered in this work. In particular, we examine how structural features of the imposed constraints, such as the number of constraints incorporated into the initialization and the size of the constraint sets, affect the resulting resource requirements. The resource metrics considered here include the total gate count, the circuit depth, and the number of two-qubit gates. The total gate count serves as a measure of circuit complexity, the circuit depth reflects the computation time, and the number of two-qubit gates provides a practical indicator of error sensitivity in experimental implementations.

Throughout this resource analysis, we focus on two representative cases, namely the states $|D_1^\mu\rangle$ and $|GHZ_{\mu,y}^{(X)}\rangle$, which encode cardinality and parity-type constraints, respectively. Although our quantitative analysis centers on these representative examples, the underlying arguments rely only on generic features such as the reduction of the effective search space and the overhead associated with state preparation. As a result, while the explicit form of the efficiency condition may depend on the specific structure of the initial state preparation, we expect that similar criteria and analytical frameworks can be employed to assess the relative efficiency of more general forms of constraint-aware initialization.

For an initialization strategy σ , let \mathcal{S}_σ denote the cost of preparing the initial state, and O_σ the cost of implementing the oracle. Each strategy σ induces a search space F_σ , and the corresponding optimal number of queries $\kappa_{F_\sigma}^{opt}$ defined in Eq. (8) is abbreviated as κ_σ . Let \mathcal{D} denote the cost of implementing the unitary $2|0\rangle\langle 0|^{\otimes n} - \mathbf{I}$, which appears in the diffusion operator and is independent of the choice of initialization strategy. Assuming that implementing a unitary and its inverse incurs the same cost, the total resource requirement can be expressed as

$$\mathcal{R}_\sigma = \mathcal{S}_\sigma + (O_\sigma + \mathcal{D} + 2\mathcal{S}_\sigma)\kappa_\sigma, \quad (20)$$

where the first term corresponds to the one-time cost of state preparation, while the second term accounts for repeated applications of the oracle and both the forward and inverse state preparation operators in each query. In practice, the overall cost may be further reduced through optimizations such as commuting operations. However, adopting the expression in Eq. (20) provides a consistent and transparent basis for comparing the relative efficiency of different initialization strategies. We say that strategy τ is more efficient than strategy σ (with respect to a given metric) if $\mathcal{R}_\tau < \mathcal{R}_\sigma$.

To compare different initialization strategies σ and τ , we make an assumption regarding the oracle implementation. Whenever the search spaces satisfy $|F_\tau| < |F_\sigma|$, we assume that the corresponding oracle costs obey $O_\tau < O_\sigma$. This assumption reflects the natural premise that an oracle typically evaluates a function over all elements within its designated domain, and therefore a smaller search space is expected to

require a lower implementation cost. Under this assumption, whenever

$$\mathcal{S}_\tau + (O_\sigma + \mathcal{D} + 2\mathcal{S}_\tau)\kappa_\tau < \mathcal{R}_\sigma, \quad (21)$$

the inequality $\mathcal{R}_\tau < \mathcal{R}_\sigma$ follows. The inequality in Eq. (21) can be rearranged to yield an explicit lower bound on the combined cost of implementing O_σ and \mathcal{D} :

$$O_\sigma + \mathcal{D} > \left(\frac{2\kappa_\tau + 1}{\kappa_\sigma - \kappa_\tau} \right) (\mathcal{S}_\tau - \mathcal{S}_\sigma) - 2\mathcal{S}_\sigma. \quad (22)$$

The criterion in Eq. (22) will be used to analyze the resource requirements of the proposed initialization schemes.

1. Cardinality constraints

Let us first consider the case of cardinality constraints and analyze how the incremental incorporation of disjoint constraint sets influences the overall resource requirement. To this end, we introduce a sequence of strategies σ_i , where σ_0 corresponds to the standard uniform initialization without constraints, and σ_i denotes the strategy obtained by incorporating i disjoint constraint sets into the initial state preparation. Each successive strategy σ_{i+1} is constructed by adding one additional disjoint constraint set of size μ_{i+1} to σ_i , and we derive conditions under which σ_{i+1} yields a lower resource cost than σ_i . The following proposition formalizes the comparison for the case in which the newly added constraint set is prepared as a Dicke state $|D_1^{\mu_{i+1}}\rangle$.

Proposition 1. Suppose that $|F_{\sigma_i}| \geq 64|S|$, where $|S|$ is the number of solutions, and that the additional disjoint constraint set incorporated in σ_{i+1} is represented by $|D_1^\mu\rangle$, where we simply denote μ_{i+1} by $\mu \geq 2$. If

$$O_{\sigma_i} + \mathcal{D} > \left(\frac{24\pi}{21\sqrt{\frac{2\mu}{\mu} - 8\pi}} \right) (\mathcal{S}_{\sigma_{i+1}} - \mathcal{S}_{\sigma_i}) - 2\mathcal{S}_{\sigma_i}, \quad (23)$$

then strategy σ_{i+1} is more efficient than strategy σ_i . In particular, when the Dicke state $|D_1^\mu\rangle$ is prepared using the circuit shown in Figure 2(a), the sufficient condition simplifies to

$$O_{\sigma_i} + \mathcal{D} \geq 67, \quad (24)$$

which guarantees that strategy σ_{i+1} is more efficient than strategy σ_i .

Proof. For $\mu \geq 2$, adding a disjoint constraint set prepared as $|D_1^\mu\rangle$ implies

$$\frac{|F_{\sigma_i}|}{|F_{\sigma_{i+1}}|} = \frac{2^\mu}{\mu} \geq 2, \quad (25)$$

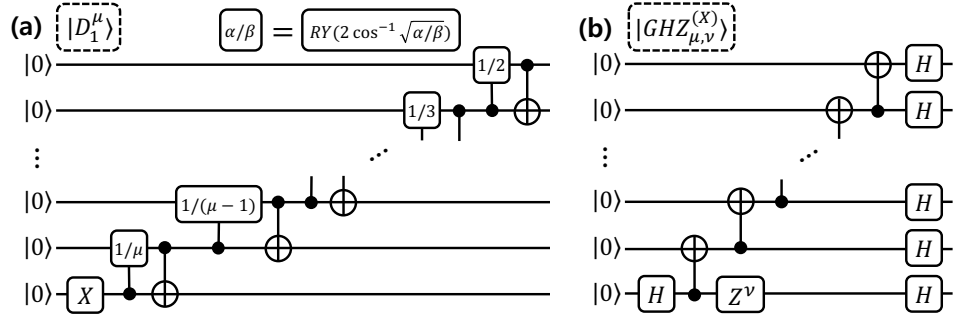


FIG. 2: (a) Quantum circuit for preparing $|D_1^\mu\rangle$ on μ qubits. (b) Quantum circuit for preparing $|GHZ_{\mu,\nu}^{(X)}\rangle$ on μ qubits. From the circuits, the total gate count, the two-qubit gate count, and the circuit depth are $2\mu - 1$, $2\mu - 2$, and $2\mu - 1$ for (a), and $2\mu + 1$, $\mu - 1$, and $\mu + 1$ for (b), respectively.

and hence $\mathcal{O}_{\sigma_{i+1}} < \mathcal{O}_{\sigma_i}$ under our oracle cost assumption. Suppose that $|F_{\sigma_i}| \geq 64|S|$. Then we have

$$\begin{aligned} \frac{2\kappa_{\sigma_{i+1}} + 1}{\kappa_{\sigma_i} - \kappa_{\sigma_{i+1}}} &\leq \frac{3\pi \sqrt{\frac{|F_{\sigma_i}|}{|S|}} \cdot \frac{\mu}{2^\mu}}{4\kappa_{\sigma_i} - \pi \sqrt{\frac{|F_{\sigma_i}|}{|S|}} \cdot \frac{\mu}{2^\mu}} \\ &\leq \frac{24\pi}{21 \sqrt{\frac{2^\mu}{\mu}} - 8\pi}, \end{aligned} \quad (26)$$

where the first inequality follows from $x \leq \arcsin x$ for $0 \leq x \leq 1$, applied to $x = \sqrt{|S|/|F_{\sigma_{i+1}}|}$. Since the assumption $|F_{\sigma_i}| \geq 64|S|$ implies $\sqrt{|S|/|F_{\sigma_i}|} \leq 1/8 < 0.17$, the second inequality follows from the bound $\arcsin x \leq 8\pi x/25$ for $0 \leq x \leq 0.17$. We also note that the conditions $\mu \geq 2$ and $|F_{\sigma_i}| \geq 64|S|$ ensure that all denominators appearing above are strictly positive. Combining this bound with the previously derived resource comparison criterion yields a simpler sufficient condition in Eq. (23).

Under the specific implementation where the Dicke state $|D_1^\mu\rangle$ is prepared using the circuit shown in Figure 2(a), the additional cost incurred by incorporating one more constraint set satisfies

$$\mathcal{S}_{\sigma_{i+1}} - \mathcal{S}_{\sigma_i} \leq 2\mu, \quad (27)$$

for each of the considered resource metrics, such as the total gate count, the circuit depth, and the number of two-qubit gates. Therefore, we obtain a sufficient condition for this specific implementation,

$$\mathcal{O}_{\sigma_i} + \mathcal{D} \geq \frac{48\pi\mu}{21 \sqrt{\frac{2^\mu}{\mu}} - 8\pi}, \quad (28)$$

where we omit the negative term $-2\mathcal{S}_{\sigma_i}$. It can be shown that the right-hand side decreases monotonically for $\mu \geq 2$, and its value at $\mu = 2$ is approximately 66.1. This completes the proof. \square

An interesting observation is that the cost \mathcal{D} of implementing $2|\langle 0\rangle\langle 0|^{ \otimes n} - \mathbf{I}$ alone is typically sufficient to satisfy the inequality in Eq. (24), even without taking the oracle construction into account. In practice, \mathcal{D} is dominated by the

implementation of the multi-controlled Z gate (which can be expressed using Hadamard gates and a multi-controlled X gate). Decomposing this component using a standard ancilla-assisted construction [26] yields gate counts and circuit depths that readily exceed the threshold value of 67 even for a relatively small number of qubits. The same conclusion holds for ancilla-free decompositions, which generally require substantially higher resource costs [27]. Consequently, for cardinality constraints, incorporating additional disjoint constraints generically leads to improved overall resource efficiency. Notably, even when only a single constraint set is used, the resulting initialization strategy can outperform the standard approach, highlighting that effectively exploiting readily available constraints can be practically meaningful without exhaustive constraint coverage.

We next study how the size of an additional constraint set affects resource efficiency with $|D_1^\mu\rangle$. In particular, we show that incorporating a larger constraint set can further reduce the total resource cost, as formalized in the following proposition.

Proposition 2. *Consider two strategies σ and σ' that differ only in the size of the additional constraint set, which is represented by $|D_1^\mu\rangle$ for σ and $|D_1^{\mu+1}\rangle$ for σ' , where $\mu \geq 2$. Suppose that $|F_\sigma| \geq 100|S|$, where $|S|$ denotes the number of solutions. If*

$$O_\sigma + \mathcal{D} > \left(\frac{120\pi}{109 \sqrt{\frac{2\mu}{\mu+1}} - 40\pi} \right) (\mathcal{S}_{\sigma'} - \mathcal{S}_\sigma) - 2\mathcal{S}_\sigma, \quad (29)$$

then strategy σ' is more efficient than strategy σ . In particular, when the Dicke state $|D_1^\mu\rangle$ is prepared using the circuit shown in Figure 2(a), the sufficient condition simplifies to

$$O_\sigma + \mathcal{D} \geq 97, \quad (30)$$

for $\mu \geq 3$.

Proof. The inequality in Eq. (29) follows from an argument analogous to the proof of Proposition 1, by repeating the same steps under the conditions $|F_\sigma| \geq 100|S|$ and

$$\frac{|F_\sigma|}{|F_{\sigma'}|} = \frac{2\mu}{\mu+1}. \quad (31)$$

When the Dicke state $|D_1^\mu\rangle$ is prepared using the circuit shown in Figure 2(a), substituting $S_{\sigma'} - S_{\sigma} = 2$ yields a further simplified sufficient condition,

$$O_{\sigma} + \mathcal{D} > \frac{240\pi}{109\sqrt{\frac{2\mu}{\mu+1}} - 40\pi}. \quad (32)$$

The right-hand side is decreasing for $\mu \geq 2$, and its value drops sharply when μ increases from 2 to 3, after which the decrease becomes more gradual. Evaluating the bound at $\mu = 3$ provides a simple and conservative sufficient condition that holds for all $\mu \geq 3$, yielding the inequality in Eq. (30). \square

Proposition 2, established for the $|D_1^\mu\rangle$ -based initialization, indicates that incorporating a larger constraint set can improve resource efficiency. Accordingly, the preprocessing in Algorithm 1 allows us to increase the attainable resource advantage even in the worst-case scenario where only a single constraint set is ultimately used. In other words, although the preprocessing strategy may not be optimal, it remains meaningful as a simple baseline that strengthens the resource advantage in a conservative setting.

2. Parity-type constraints

In analogy to the discussion of cardinality constraints in the previous subsection, we examine how parity-type constraints affect the resource cost of the initialization. A key difference is that a parity constraint implemented via a GHZ-type state $|GHZ_{\mu,\nu}^{(X)}\rangle$ always reduces the search space by half, independent of the constraint set size μ . As a result, increasing μ does not yield any further reduction of the search space, but instead incurs a higher circuit cost. It therefore follows that, for parity-type constraints, applying constraints on smaller subsets of qubits is generally more efficient in terms of overall resource cost.

We now examine how the number of imposed parity-type constraints affects the overall resource requirements. As before, we consider a sequence of strategies σ_i , where σ_0 denotes the standard initialization and each successive strategy incorporates one additional disjoint constraint set of size μ . Adding such a set via $|GHZ_{\mu,\nu}^{(X)}\rangle$ halves the search space, that is, $|F_{\sigma_i}|/|F_{\sigma_{i+1}}| = 2$, and thus reduces the oracle cost under our assumption. Meanwhile, when $|GHZ_{\mu,\nu}^{(X)}\rangle$ is implemented using the circuit in Figure 2(b), then we have $S_{\sigma_{i+1}} - S_{\sigma_i} \leq 2\mu + 1$. Hence, by applying the same comparison argument as in Proposition 1, we obtain the following result.

Proposition 3. Suppose that $|F_{\sigma_i}| \geq 64|S|$, where $|S|$ is the number of solutions, and that the additional disjoint constraint set incorporated in σ_{i+1} is represented by $|GHZ_{\mu,\nu}^{(X)}\rangle$. If

$$O_{\sigma_i} + \mathcal{D} > \left(\frac{24\pi}{21\sqrt{2} - 8\pi} \right) (S_{\sigma_{i+1}} - S_{\sigma_i}) - 2S_{\sigma_i}, \quad (33)$$

then strategy σ_{i+1} is more efficient than strategy σ_i . When preparing $|GHZ_{\mu,\nu}^{(X)}\rangle$ using the circuit in Figure 2(b), we have

a simplified sufficient condition:

$$O_{\sigma_i} + \mathcal{D} > \frac{24\pi(2\mu + 1)}{21\sqrt{2} - 8\pi}. \quad (34)$$

The right-hand side of the inequality in Eq. (34) scales linearly with the constraint set size μ . Even so, when μ is small compared to the total number of qubits, the inequality can often be satisfied by accounting only for the cost \mathcal{D} . For larger values of μ , the condition can still be met in practice once the oracle construction cost O is taken into account. Therefore, incorporating disjoint constraint sets, even with relatively large μ , can still be advantageous in terms of overall resource efficiency.

B. Simulation results for cardinality constraints

To illustrate the effectiveness of the proposed initialization scheme, we consider the exact-cover problem as a representative combinatorial benchmark. Given a collection $\mathcal{A} = \{A_1, A_2, \dots, A_n\}$ of subsets of a universal set $U = \{u_1, u_2, \dots, u_m\}$, a subcollection $\mathcal{A}' \subseteq \mathcal{A}$ is said to form an exact-cover of U if it satisfies the following two conditions:

(i) Any two distinct subsets $A_i, A_j \in \mathcal{A}'$ are disjoint:

$$A_i \cap A_j = \emptyset.$$

(ii) The union of all subsets in \mathcal{A}' covers the entire set U :

$$\bigcup_{A_i \in \mathcal{A}'} A_i = U.$$

The objective is to find such a subcollection \mathcal{A}' among the 2^n possible choices.

Equivalently, the problem can be formulated in terms of a binary string $x = x_1 x_2 \dots x_n \in \{0, 1\}^n$, where $x_i = 1$ indicates that subset A_i is selected. For each $j \in \{1, 2, \dots, m\}$, we define

$$C_j = \{i \mid u_j \in A_i\}, \quad (35)$$

the set of indices of subsets that contain u_j . The exact-cover condition then requires that

$$\sum_{i \in C_j} x_i = 1, \quad j = 1, \dots, m, \quad (36)$$

which enforces that each element is covered by exactly one selected subset.

Suppose that, after performing the classical preprocessing described in Algorithm 1 and reordering the qubit indices, we obtain a collection of disjoint subsets C'_1, \dots, C'_t and reduced subsets R'_{t+1}, \dots, R'_s derived from overlapping constraints. Let k_j denote the number of qubits in the j -th subset. For each disjoint subset C'_j , we prepare the Dicke state $|D_1^{k_j}\rangle$ acting on the qubits $\mathbf{q}_{C'_j}$ to represent the corresponding constraint. For

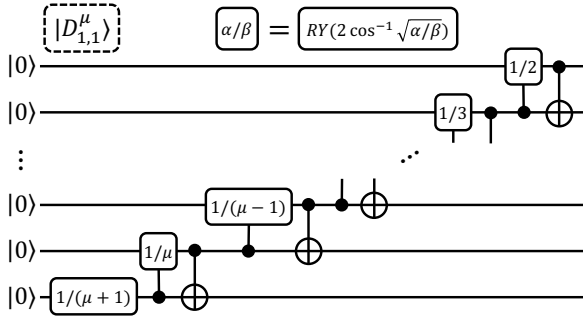


FIG. 3: Quantum circuit for preparing $|D_{1,1}^\mu\rangle$ on μ qubits.

each reduced subset R'_j , we employ the state $|D_{1,1}^{k_j}\rangle$ defined in Eq. (13), whose explicit form is

$$|D_{1,1}^{k_j}\rangle_{\mathbf{q}_{R'_j}} = \frac{1}{\sqrt{k_j+1}} |00\cdots 0\rangle_{\mathbf{q}_{R'_j}} + \frac{\sqrt{k_j}}{\sqrt{k_j+1}} |D_1^{k_j}\rangle_{\mathbf{q}_{R'_j}}. \quad (37)$$

The state $|D_{1,1}^{k_j}\rangle$ can be prepared using the circuit shown in Figure 3.

We now look at the following example of the exact-cover problem. Let $U = \{1, 2, 3, 4, 5, 6, 7\}$ and the collection of subsets be given as

$$\begin{aligned} A_1 &= \{1, 5\}, \quad A_2 = \{1, 3, 6\}, \quad A_3 = \{1, 2, 5\}, \\ A_4 &= \{1, 7\}, \quad A_5 = \{3, 4\}, \quad A_6 = \{4, 6\}, \quad A_7 = \{2, 4, 5\}, \\ A_8 &= \{2, 7\}, \quad A_9 = \{6, 7\}, \quad A_{10} = \{3, 5, 7\}. \end{aligned} \quad (38)$$

This instance admits a unique exact-cover, given by $\mathcal{A}' = \{A_3, A_5, A_9\}$, so that $|S|=1$. From the subsets in Eq. (38), the corresponding constraint sets are constructed according to Eq. (35) as

$$\begin{aligned} C_1 &= \{1, 2, 3, 4\}, \quad C_2 = \{3, 7, 8\}, \quad C_3 = \{2, 5, 10\}, \\ C_4 &= \{5, 6, 7\}, \quad C_5 = \{1, 3, 7, 10\}, \\ C_6 &= \{2, 6, 9\}, \quad C_7 = \{4, 8, 9, 10\}. \end{aligned} \quad (39)$$

Applying the classical preprocessing procedure described in Algorithm 1, we first identify disjoint sets that will be used to construct the circuit for initialization. When the threshold parameter $\eta_{\text{th}} = 0$, only strictly disjoint sets are allowed, and the preprocessing selects

$$C'_1 = C_1, \quad C'_2 = C_4. \quad (40)$$

When the threshold is relaxed to $\eta_{\text{th}} = 1$, a small degree of overlap is permitted, which allows an additional set to be obtained as

$$R'_3 = C_7 \setminus (C_1 \cup C_4) = \{8, 9, 10\}. \quad (41)$$

The initial quantum state is then constructed by preparing Dicke states on the subsystems corresponding to C'_1 and C'_2 , while the subsystem associated with R'_3 is prepared according to the quantum state of the form in Eq. (37).

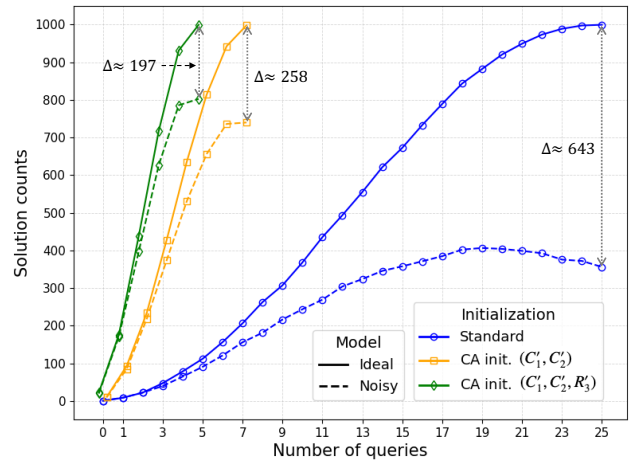


FIG. 4: Comparison of the solution counts for the exact-cover instance in Eq. (38) under different initialization strategies. The standard uniform initialization is compared with two constraint-aware initialization (CA init.) schemes incorporating (C'_1, C'_2) and (C'_1, C'_2, R'_3) , respectively. Solid (dashed) curves correspond to the ideal (noisy) model, where depolarizing noise with error rates of 10^{-5} and 10^{-4} is applied to one- and two-qubit gates. Each data point is obtained by averaging over 20 independent circuit executions, each consisting of 1000 measurement shots. Bidirectional arrows indicate the difference in the solution counts between the ideal and noisy models, evaluated at the optimal number of queries for each initialization scheme.

We perform simulations using IBM's Qiskit, an open-source software development kit for quantum circuit design and simulation [28]. The oracle operator is assumed to be ideal to reduce simulation overhead and to focus on the resource impact of the initialization and diffusion components. We note, however, that oracles for the exact-cover problem can be explicitly constructed using existing approaches, such as those proposed by Gilliam *et al.* [8] and Jiang *et al.* [21]. The operator $2|0\rangle\langle 0|^{\otimes n} - \mathbf{I}$ is implemented using the Hadamard gate H , Pauli-X and Pauli-Z gates, together with a multi-controlled X gate [26, 29]. When simulating the noisy model, the multi-controlled X gate is further decomposed into one- and two-qubit gates using the transpilation routines provided by Qiskit, which generate a circuit over the gate set $\{RZ, H, CNOT\}$. To assess the effect of noise on the performance of different initialization strategies, we consider a depolarizing noise model applied to all operations except for the oracle operator. Specifically, depolarizing noise with error rates of 10^{-5} and 10^{-4} is applied to one- and two-qubit gates, respectively. For each value of the query number, the circuit is executed 20 times, each run consisting of 1000 measurement shots. The reported results correspond to the average number of measurements yielding a solution state.

Figure 4 shows the solution counts as a function of the number of queries for the exact-cover instance defined in Eq. (38), obtained using the standard uniform initialization and two constraint-aware initialization strategies. The first constraint-aware strategy incorporates only the disjoint constraint sets (C'_1, C'_2) , while the second additionally includes the reduced

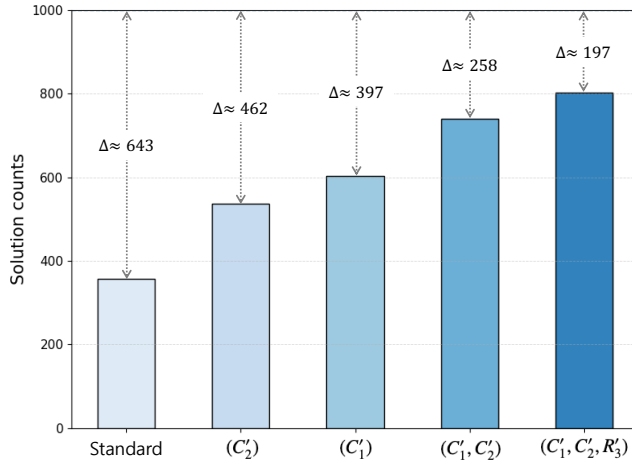


FIG. 5: Difference in solution counts between the ideal and noisy models, evaluated at the respective optimal number of queries for different initialization strategies, where the bars show the solution counts in the noisy model and Δ denotes the corresponding difference. All simulation settings are the same as in Figure 4. The strategies include the standard uniform initialization and several constraint-aware initializations incorporating single constraint sets (C'_2) and (C'_1) , as well as multiple constraint sets obtained through preprocessing, namely (C'_1, C'_2) and (C'_1, C'_2, R'_3) .

set R'_3 derived from overlapping constraints. For each initialization strategy, results are shown for both the ideal and noisy models. In the standard initialization, the corresponding optimal number of queries is 25, whereas the first constraint-aware strategy reduces the optimal number of queries to 7, and the second strategy further reduces it to 5. Although the constraint-aware initialization increases the circuit complexity associated with initial state preparation and the diffusion operator, the substantial reduction in the optimal number of queries leads to improved robustness against noise at the respective optimal query numbers.

Figure 5 extends the comparison by examining the difference in solution counts between the ideal and noisy models at the respective optimal number of queries for a broader set of initialization strategies. In addition to the standard uniform initialization and the two constraint-aware schemes based on (C'_1, C'_2) and (C'_1, C'_2, R'_3) , which were discussed earlier, we also include constraint-aware initializations incorporating only a single constraint set, namely (C'_2) and (C'_1) . These two cases correspond to reduced search spaces of size 3/8 and 1/4 of the reference space of size 2^{10} , respectively, which result in optimal query numbers of 15 and 12. As shown in Figure 5, the solution counts obtained in the noisy model increase as we move from the standard initialization to constraint-aware strategies that incorporate larger constraint sets and additional disjoint constraint sets. These results provide supporting evidence for the constraint selection strategy adopted in Algorithm 1, where larger constraint sets are prioritized and the procedure is designed to identify as many disjoint constraint sets as possible.

Importantly, Figure 5 shows that even in unfavorable preprocessing scenarios where only a single constraint set is iden-

tified, the corresponding constraint-aware initialization still yields a noticeable improvement over the standard uniform initialization. This suggests that the proposed preprocessing-guided initialization offers a systematic and practically feasible way to incorporate constraints. While incorporating additional constraints, including non-disjoint ones, may further improve performance, it is nontrivial to design a systematic initialization that directly incorporates non-disjoint constraint sets in a systematic manner. Our preprocessing instead relaxes overlaps by extracting reduced subsets that can be implemented in the initialization, and the simulation results support the effectiveness of this approach. Moreover, identifying a large number of disjoint constraint sets is itself challenging. Accordingly, we adopt a greedy preprocessing strategy that does not aim to be optimal but provides a simple and implementable baseline that already delivers a clear performance advantage in our simulations.

C. Simulation results for parity-type constraints

We now introduce a variant of the exact-cover problem to illustrate the incorporation of parity-type constraints through GHZ-type initialization. The universal set U and the collection of subsets $\{A_i\}$ are taken to be the same as in Sec. III B. In contrast to the standard exact-cover formulation, we do not require the selected subsets to be disjoint. Instead, we require each element of U to be covered exactly twice. We assign weights α_i to the subsets such that when A_i is selected, it contributes α_i to the coverage count of each element it contains. We set $\alpha_i = 2$ for $i \in \{3, 6, 10\}$ and $\alpha_i = 1$ otherwise. Introducing binary variables $x_i \in \{0, 1\}$, this condition is expressed as

$$\sum_{i \in C_j} \alpha_i x_i = 2, \quad j = 1, \dots, 7, \quad (42)$$

and this instance admits a unique solution given by $\mathcal{A}' = \{A_1, A_2, A_5, A_7, A_8, A_9\}$.

Using the definition of $\hat{C}_j = \{i \in C_j | \alpha_i \text{ is odd}\}$, we obtain

$$\begin{aligned} \hat{C}_1 &= \{1, 2, 4\}, & \hat{C}_2 &= \{7, 8\}, & \hat{C}_3 &= \{2, 5\}, & \hat{C}_4 &= \{5, 7\}, \\ \hat{C}_5 &= \{1, 7\}, & \hat{C}_6 &= \{2, 9\}, & \hat{C}_7 &= \{4, 8, 9\}. \end{aligned} \quad (43)$$

Accordingly, by applying the preprocessing step in Algorithm 2, we identify disjoint sets $C'_1 = \hat{C}_2$ and $C'_2 = \hat{C}_3$. We then implement the GHZ-type initialization on the qubit registers associated with these constraint sets. Since two disjoint parity-type constraint sets are incorporated, the effective search space is reduced by a factor of $2^2 = 4$, which yields an optimal number of queries of 12 for this instance.

Figure 6 presents the simulation results obtained under the same settings as in Sec. III B. We plot the solution counts as a function of the number of queries for the ideal and noisy cases. The results compare three initialization strategies that include applying GHZ-type initialization to both C'_1 and C'_2 , applying it only to C'_1 , and the standard uniform initialization. As in the cardinality case, incorporating additional constraint information leads to improved performance under noise. Even

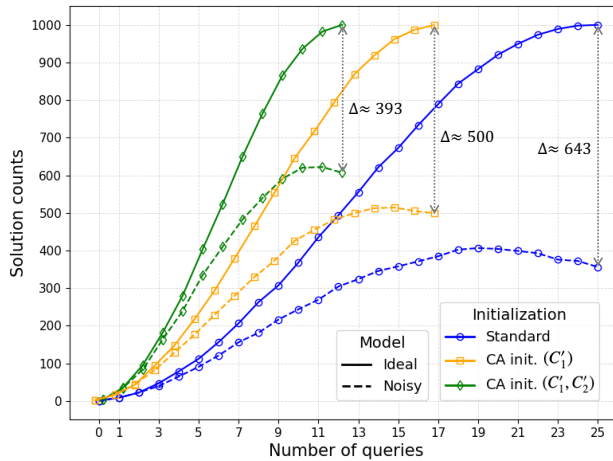


FIG. 6: Comparison of the solution counts under different initialization strategies for parity-type constraints. The standard uniform initialization is compared with two GHZ-type initialization incorporating (C'_1) and (C'_1, C'_2) , respectively. Consistent with the cardinality case, incorporating additional parity-type constraint information improves performance under noise, and even incorporating a single constraint set yields a clear advantage over the uniform initialization.

incorporating a single parity-type constraint set already yields a clear improvement over the standard uniform initialization. Together with the results in Sec. III B, this confirms that the proposed constraint-aware initialization framework can systematically exploit different types of linear constraints to improve practical performance.

IV. CONCLUSION

In this work, we presented a systematic framework for constraint-aware initialization in Grover's algorithm applied to combinatorial problems with linear constraints, which reduces the effective search space by incorporating constraint information already at the initialization step. The proposed approach combines a simple classical preprocessing step with structured initial state preparation. The preprocessing selects collections of mutually disjoint constraint sets that are jointly implementable in the initialization. For each selected set, we prepare a structured quantum state that encodes the corresponding constraint information. We use Dicke states to encode cardinality constraints and GHZ-type states to incorporate parity-type information. The overall initial state is then

constructed as a tensor product over the selected sets. We also provided a conservative circuit-level resource analysis, showing that although structured initialization introduces additional preparation costs, it can still improve overall resource efficiency in terms of gate counts and circuit depth compared to the standard uniform initialization. The practical effectiveness of the framework was further supported by numerical simulations of the exact-cover problem, demonstrating clear performance advantages, particularly in the presence of noise.

Several important directions remain for future work. While the present analysis focused on specific instances of Dicke states and GHZ-type states, more general Dicke states are known to admit polynomial-time circuit constructions [25], suggesting that similar resource-efficiency trends may extend beyond the cases considered here. In addition, the circuit implementations examined in this work are not optimized for minimal resource usage, and further improvements may be achieved through more efficient state preparation schemes. The classical preprocessing procedure introduced in this framework is likewise intended as a simple and practical baseline rather than an optimal approach, and identifying more effective preprocessing methods will be important for achieving both practical efficiency and near-optimal performance.

Another natural direction is to extend the framework beyond equality-type linear constraints to inequality constraints. Such constraints may be incorporated by preparing superpositions of Dicke states across a range of Hamming weights, which suggests that the proposed approach could be generalized to a broader class of combinatorial problems. Finally, it would be interesting to apply the proposed framework within optimization settings such as Grover adaptive search [8] and variational algorithms with the Grover mixer quantum alternating operator ansatz [22], and to evaluate its impact on practically relevant combinatorial optimization problems.

ACKNOWLEDGMENTS

This work was supported by the Institute for Information & Communications Technology Promotion (IITP) (2019-0-00003) and the Global TOP strategic Research Program of the National Research Council of Science & Technology (NST) (GTL25011-000) grant funded by the Korea government (MSIT). M.C. acknowledges support from the Korea Institute of Science and Technology Information (KISTI) (Grant No. K26L3M3C3).

[1] L. K. Grover, in *Proceedings of the twenty-eighth annual ACM symposium on Theory of computing* (1996), pp. 212–219.

[2] G. Brassard, P. Hoyer, M. Mosca, and A. Tapp, arXiv preprint quant-ph/0005055 (2000).

[3] A. Montanaro, *npj Quantum Information* **2**, 1 (2016).

[4] G. Brassard, P. Hoyer, and A. Tapp, in *Proceedings of the 25th International Colloquium on Automata, Languages, and Programming (ICALP)* (Springer, Berlin, Heidelberg, 1998), pp. 820–831.

[5] S. Aaronson and P. Rall, in *Symposium on simplicity in algorithms* (SIAM, 2020), pp. 24–32.

[6] C. Durr and P. Hoyer, arXiv preprint arXiv:quant-ph/9607014 (1996).

[7] W. P. Baritompa, D. W. Bulger, and G. R. Wood, SIAM Journal

on Optimization **15**, 1170 (2005).

[8] A. Gilliam, S. Woerner, and C. Gonciulea, Quantum **5**, 428 (2021).

[9] H. Nigatu, G. Shi, J. Li, J. Wang, G. Lu, and H. Li, IEEE Robotics and Automation Letters **10**, 13090 (2025).

[10] E. Campbell, A. Khurana, and A. Montanaro, Quantum **3**, 167 (2019).

[11] Á. Nagy, J. Park, C. Zhang, A. Acharya, and A. Khan, arXiv preprint arXiv:2311.05592 (2023).

[12] H. Ohno, Quantum Machine Intelligence **6**, 12 (2024).

[13] Y. Sano, K. Mitarai, N. Yamamoto, and N. Ishikawa, IEEE Transactions on Quantum Engineering (2024).

[14] H. Ominato, T. Ohyama, and K. Yamaguchi, IEEE Access **12**, 74619 (2024).

[15] S. A. Metwalli, F. Le Gall, and R. Van Meter, IEEE Transactions on Quantum Engineering **1**, 1 (2020).

[16] T. Mikuriya, K. Yukiyoshi, S. Fujiwara, G. T. F. de Abreu, and N. Ishikawa, arXiv preprint arXiv:2410.12181 (2024).

[17] R. H. Dicke, Physical Review **93**, 99 (1954).

[18] D. M. Greenberger, M. A. Horne, and A. Zeilinger, in *Bell's theorem, quantum theory and conceptions of the universe* (Springer, 1989), pp. 69–72.

[19] P. Vikstål, M. Grönkvist, M. Svensson, M. Andersson, G. Johansson, and G. Ferrini, Physical Review Applied **14**, 034009 (2020).

[20] A. Bengtsson, P. Vikstål, C. Warren, M. Svensson, X. Gu, A. F. Kockum, P. Krantz, C. Križan, D. Shiri, I.-M. Svensson, et al., Physical Review Applied **14**, 034010 (2020).

[21] J.-R. Jiang and Y.-J. Wang, in *2023 VTS Asia Pacific Wireless Communications Symposium (APWCS)* (IEEE, 2023), pp. 1–5.

[22] A. Bärtschi and S. Eidenbenz, in *2020 IEEE International Conference on Quantum Computing and Engineering (QCE)* (IEEE, 2020), pp. 72–82.

[23] R. Sato, K. Saito, T. Nikuni, and S. Watabe, in *2023 IEEE International Conference on Quantum Computing and Engineering (QCE)* (IEEE, 2023), vol. 2, pp. 270–271.

[24] R. Sato, C. Gordon, K. Saito, H. Kawashima, T. Nikuni, and S. Watabe, IEEE Transactions on Quantum Engineering (2025).

[25] A. Bärtschi and S. Eidenbenz, in *International Symposium on Fundamentals of Computation Theory* (Springer, 2019), pp. 126–139.

[26] M. A. Nielsen and I. L. Chuang, *Quantum Computation and Quantum Information: 10th Anniversary Edition* (Cambridge University Press, 2010).

[27] D. Maslov, Physical Review A **93**, 022311 (2016).

[28] A. Javadi-Abhari, M. Treinish, K. Krsulich, C. J. Wood, J. Lishman, J. Gacon, S. Martiel, P. D. Nation, L. S. Bishop, A. W. Cross, et al. (2024), 2405.08810.

[29] T. G. Wong, *Introduction to classical and quantum computing* (Rooted Grove Omaha, NE, USA, 2022).